

0017-9310(94)E0039-W

Interfacial fluxes at a grid-stirred diffusive interface

JOSEPH F. ATKINSON

Department of Civil Engineering, State University of New York at Buffalo, Buffalo, NY 14260, U.S.A.

(Received 17 May 1993 and in final form 24 January 1994)

Abstract—Results from a grid-mixing experiment in a diffusive thermohaline system are described. A model is proposed to separate the effects of interfacial flux and interfacial movement (entrainment) on property changes in the mixed layer and the present results for heat and salt fluxes are compared with previous studies in unstirred diffusive systems. Comparison of an eddy time-scale and a time-scale for development of instability in the interfacial boundary layers suggests a means of determining whether stirring or double-diffusive instability controls the interfacial transports. For the present conditions there was a negligible effect of diffusive stratification on entrainment rates, and interfacial fluxes were increased by the stirring. It is suggested that the ratio R_F/R_p , where R_F is the interfacial flux ratio and R_p is the interfacial stability ratio, should be a function of the overall bulk Richardson number, Ri .

1. INTRODUCTION

MIXING AND property fluxes across a density interface have received considerable attention, in large part due to their importance in affecting the stratification of fluid systems. Modeling the oceanic mixed layer, the atmospheric boundary layer, stratification of water storage reservoirs or the operation of salt gradient solar ponds are just a few examples where a knowledge of interfacial mixing is needed. Fluxes of fluid properties such as heat and dissolved mass must be known, as well as movement of the interface itself. These all affect the overall structure and quality of a given fluid body.

The present work is concerned with a “diffusive” thermohaline system, where salinity is stably stratified while the temperature distribution is unstable. This type of stratification is found in various systems such as oceans, bottom-heated saline lakes, Antarctic lakes, liquified natural gas storage tanks and solar ponds. A number of models have been proposed for calculating the property fluxes across a diffusive interface, starting with the pioneering work of Turner [1], who heated a salinity gradient from below and deduced relationships for the heat and salt fluxes across the interface which developed. His results indicated that the buoyancy flux ratio, R_F , was a constant equal to about 0.15 when the interfacial stability ratio, R_p , was between 2 and 7. These parameters are defined as:

$$R_F = \frac{\beta F_S \rho_0 c_p}{\alpha F_H} \quad R_p = \frac{\beta \Delta S}{\alpha \Delta T} \quad (1)$$

where F_S = interfacial salt flux, F_H = interfacial heat flux, ΔS = interfacial salinity step, ΔT = interfacial temperature step, $\alpha = -1/\rho_0(\partial\rho/\partial T)$ = thermal expansion coefficient, $\beta = 1/\rho_0(\partial\rho/\partial S)$ = saline

expansion coefficient, ρ = density, ρ_0 = reference value for ρ , and c_p = specific heat. The temperature and salinity steps are defined as positive when the property increases downward. Turner's results also showed that R_F increased sharply when R_p was less than 2. This was interpreted as being a result of increased turbulent transport as the interfacial conditions became less stable.

Subsequent studies have suggested that R_F should depend on the ratio of molecular diffusivities, or Lewis number, $\tau = k_S/k_T$, where k_S = salt diffusivity, and k_T = heat diffusivity. Turner *et al.* [2] deduced $R_F = \tau^{1.2} R_p$, while Shirtcliffe [3] found $R_F = \tau^{1.2}$. Linden and Shirtcliffe [4] developed a mechanistic model of the interface which also supported $R_F = \tau^{1.2}$. Their model was based on the process of development of an unstable boundary layer due to the faster diffusion of heat, compared with salt. Fernando [5] adopted a similar approach, except he argued that convective motions in the mixed layers scour the developing boundary layers before instability develops. His model results in $R_F = \tau^{1.2} R_p$, as above.

Relatively few studies have looked specifically at the problem of entrainment in diffusive systems, compared with the numerous studies of mixing at density interfaces in singly-stratified systems (see ref. [5] for a recent review). Oscillating grid experiments have been useful in gaining general understanding of interfacial turbulent mixing, with some of the important studies in this area reported in refs. [6–12]. Major problems addressed in these studies concern the physical entrainment mechanism and the proper form of the entrainment law:

$$E = \frac{u_e}{u_i} \propto Ri^{-n} \quad (2)$$

NOMENCLATURE

c_p	constant pressure specific heat	z_g	distance below mean grid position.
E	dimensionless entrainment rate	Greek symbols	
f	grid oscillation frequency	α	thermal expansion coefficient
F	interfacial flux	β	saline expansion coefficient
g	gravity	δ	interfacial thickness
h	mixed layer depth	κ	molecular thermal conductivity, or transfer coefficient
H	heat content per unit volume	λ	ratio of eddy and convective velocities
H_{sp}	idealized interfacial heat flux	ν	kinematic viscosity
k	molecular diffusivity	ρ	density
l	length scale	τ	Lewis number, ratio of diffusivities
l_i	ratio of interfacial thicknesses	ζ	ratio of depths.
n	exponent	Subscripts	
Pe	Peclet number	c	convective scale
R_F	buoyancy flux ratio	d	diffusive scale
R_p	interfacial stability ratio	e	entrainment value
Ra_c	critical Rayleigh number	H	heat
Ri	bulk Richardson number	o	reference value
s	grid oscillation stroke	S	salinity value
S	salinity	T	heat, or temperature value
t	time	l	turbulence scale.
t_e	eddy time-scale		
T	temperature		
u	velocity scale		
∇	volume		

where $u_c = dh/dt =$ rate of mixed layer growth, $h =$ mixed layer depth, $u_t =$ turbulent velocity scale and Ri is a bulk Richardson number defined by:

$$Ri = g \frac{\Delta\rho}{\rho_o} \frac{l_i}{u_t^2}, \quad (3)$$

where $g =$ gravitational acceleration, $\Delta\rho =$ interfacial density step and $l_i =$ turbulent length scale. Different values for the exponent n in (2) have been reported, ranging between about 1 and 1.75, with some dependence on whether heat or salt was used as the stratifying agent.

Crapper [13] studied grid-mixing in a diffusive system for cases with relatively low R_p . His results showed higher values for R_F than in unstirred systems and also that F_S was increased when ΔT was higher. This latter result is consistent with other expressions derived for F_S [14]. Other studies performed to evaluate entrainment and mixing in diffusive systems include Linden's [15] analysis, which incorporated the entrainment formula (2) with $n = 1.5$, to predict the relationship between R_F and R_p resulting from Turner's data [1]. Murota and Michioku [16] heated a stable salt gradient from below and measured the growth of the developing mixed layer. They defined the convective velocity scale u_c , associated with instability driven by the bottom heating, as the scaling velocity (u_t) and obtained an entrainment relationship similar to (2), with n varying between 1 and 1.5.

Additional models of convective-driven mixing in a

diffusive system have been proposed [17–19]. Witte and Newell [18] developed a thermal burst model based on development of boundary-layer instability, similar to the model of Linden and Shirtcliffe [4]. They assumed that the unstable fluid in the boundary layers is incorporated into the mixed layer, thus increasing the layer depth at a rate interpreted as the entrainment velocity. There are several difficulties with this model, as pointed out in [17, 19], perhaps the most important one being the neglect of the role of convection in the bottom layer. Hull and Mehta [17] performed a mathematical stability analysis incorporating the effects of periodic temperature variations on the boundary of a diffusive layer, meant to simulate the effect of thermals rising from the heated bottom. While some interesting results were presented, interfacial movement was not specifically addressed. Zangrando and Fernando's model [19] is based on the development of salinity and temperature diffusive boundary layers, assuming that they become scoured by turbulent eddies before instability can develop [20]. Therefore, interfacial fluxes and movement depend on an eddy time-scale rather than an instability time-scale.

In the present study we examine the entrainment and interfacial fluxes of heat and salt resulting at a grid-stirred diffusive interface and present results which extend the parameter range considered in ref. [13]. The results are interpreted in the context of previous studies as reviewed above, particularly the inter-

facial flux models proposed for diffusive interfaces. A procedure is first developed to distinguish between interfacial and entrainment fluxes. Results for the parameter ranges considered here indicate: (1) a negligible effect of double-diffusive stratification on entrainment rates; and (2) increased interfacial fluxes of heat and salt, compared with unstirred systems. These increases are explained in terms of reduced interfacial thicknesses, with the fluxes still consistent with molecular diffusion. A time-scale comparison is also suggested as a means of determining when double-diffusive effects would be expected to become important.

2. EXPERIMENTS

Experiments were conducted in a rectangular tank made of 1.3 cm thick plate glass with 10.2 cm of styrofoam insulation on all sides. An outer jacket of 0.8 cm plywood held the insulation in place and further minimized heat losses. The inside dimensions of the tank were 41.3 cm square in plan view and 50.8 cm high. Windows were cut in the front and back which could be removed for short periods for observation. During an experiment the mean grid position was about 4 cm below the water surface and insulation was floated on the surface to further reduce heat loss. Two-layer stratification was used, with the initial interface position about 7 or 8 cm below the grid. The basic apparatus is sketched in Fig. 1.

The experiments were conducted in a "run-down" fashion, that is, there was no heating of the bottom layer once the tank was filled and there was also no attempt to maintain a constant interfacial position. For each test the bottom layer was first filled with solution of the desired salinity and heated to the desired temperature. The upper layer was then carefully poured on top. Some diffusion of the interface was inevitable during the filling process, but it was quickly sharpened once the grid was started. All measurements reported here correspond with an interfacial position 10 cm below the mean grid position

(center of stroke). This depth represents the minimum distance required in order to insure turbulent motions [21], but is also such that u_c is not too small. This procedure eliminates possible problems associated with ambiguities in estimating the turbulent velocity and length-scales [11]. Also, in order to reduce the number of variables, all tests were conducted with constant grid oscillation stroke and frequency, $s = 1$ cm and $f = 5$ Hz, respectively. Thus, all results reported here have the same u_1 and l_1 values.

The grid was composed of square plexiglass strips, 0.95 cm on a side and 40.5 cm long, joined together in a square array with 5 cm spacing. The middle of the grid was reinforced to make the connection with the driving rod as rigid as possible and the overall geometric solidity of the grid was 39%. The motor, eccentric wheel and joint connections were suspended above the tank and the only physical connection to the tank was between the driving rod and the Teflon bearings in the tank top.

Temperature and salinity values were measured with a thermistor and conductivity probe mounted at the end of a stainless steel tube passing through a hole in the bottom of the tank. The tube was connected to a point gage and could be moved to record values at different vertical positions. A potentiometer provided probe position data. Details of the salinity and temperature probe construction and calibrations are given in ref. [22]. Data accuracy is estimated to be $\pm 0.1^\circ\text{C}$ for temperature and $\pm 0.1\%$ (by weight) for salinity. An equation of state was used to calculate density as a function of T and S . This relationship was based on least-squares fitting of data from ref. [23]. A separate series of tests was performed in which ρ was measured directly using a hydrometer in solutions of varying T and S . Values calculated with the equation of state were found to be within 1–2% of measured values. The calculations were also nearly identical to results from ref. [13], which were based on a multi-regression fit to standard tabulated values.

Deepening of the mixed layer was monitored for each test by observing interfacial movement over time. Interfacial positions were determined either by calculating the location of the maximum density gradient from the temperature and salinity probe output or by flow observation, with dye or shadowgraph techniques used to identify the interface. The flow visualization procedure tended to produce somewhat smoother results since each reading was visually averaged, whereas the probe output reflected more of a local value and was subject to perturbations induced by deflections of the interface. It was found that simple power-law curves could usually be fitted to the interfacial position data and u_c was calculated as the slope of those curves at any given value of $z_g =$ distance from grid. Following a suggestion by Nokes [11] to evaluate more accurately correct values for u_c , only those data centered around the desired value of $z_g = 10$ cm were used in these calculations. Based on the variability obtained when using different points in

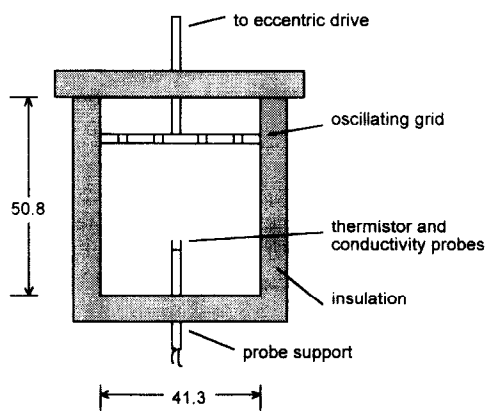


FIG. 1. Schematic of experimental apparatus; all dimensions are in cm.

this analysis, values for u_c are estimated to have an average accuracy of about ± 20 –30%.

A laser-Doppler anemometer (LDA) was used to measure velocities. Vertical profiles of the horizontal velocity component were obtained at several different locations within the tank and averaged to determine the desired scaling velocity. These data were measured without density stratification in order to avoid problems with index of refraction fluctuations. That this procedure provides appropriate scaling quantities for the entrainment tests was suggested by McDougall [10] and later confirmed by Carruthers and Hunt [24]. The measured velocity profiles were reported previously [21], with a reasonable fit to the data given by:

$$\frac{u_1}{f_s} = 0.71 \left(\frac{z_g}{s} \right)^{-1} \quad (4)$$

For the present experimental conditions, $u_1 = 0.37 \text{ cm s}^{-1}$ at $z_g = 10 \text{ cm}$. The variability of u_1 values obtained for the different profile positions was about $\pm 30\%$. The accuracy of the depth measurements is estimated to be $\pm 2 \text{ mm}$ (2%). Values for l_1 have been shown to be proportional to z_g , both from direct measurements of the autocorrelation length scale based on hot-film data [25] and by inference from LDA data [8], with the proportionality coefficient equal to 0.1.

3. RESULTS

A summary of experimental results is shown in Tables 1 and 2 for salt and diffusive stratification, respectively. Figure 2 shows a plot of E as a function of Ri , where it can be seen that there is no apparent difference between the results for the two types of stratification. This is true even for relatively large ΔT (up to 14°C). Although the temperature step slightly modifies the density step resulting from salt strati-

fication, the salinity interface still controls movement of the interface. It might be expected that E should increase, relative to the salt-stratified results, when the buoyancy step due to temperature is increased. This implies a lower value for R_p , but also lower values for Ri , since it is based on the net interfacial density step (note that $R_p \rightarrow 1$ implies $Ri \rightarrow 0$). At low values of Ri the turbulence is relatively strong and molecular effects will be less important. Thus, there is less likelihood of any difference in entrainment results for systems with different stratifying components to be seen at low Ri (see also ref. [12]).

A least-squares analysis of the data in Fig. 2 indicates that for $Ri > 5$ the value for the exponent n in (2) is about 1.1–1.2, which is close to previous values [10, 11]. (Points corresponding to low Ri show a “flattening” of the entrainment curve, which is consistent with [12].) A least-squares regression for double-diffusive data only for the same Ri range results in a slightly lower value, $n \approx 1.0$, but this is not significantly different than the value corresponding to the full data set. Although the presence of the temperature gradient should weaken the interface locally, there is no significant effect on the rate of interfacial movement. As shown below, there is however an effect of the stirring on the interfacial fluxes of heat and salt.

Before interfacial fluxes can be evaluated, a distinction must be made between those changes in T and S of the upper layer which are due to entrainment and those due to interfacial fluxes. This is done using a model for the changes in ΔS and ΔT over time. We first consider a system consisting of two well-mixed reservoirs, one over the other, separated by a thin interface and isolated from the environment. The temperature and salinity of the lower reservoir are higher than the corresponding values in the upper reservoir. The only heat and salt transfer in the system are accomplished by interfacial diffusion or by entrainment. Further, it is assumed that mixing in the upper layer causes entrainment and $u_e = dh_u/dt = -dh_l/dt > 0$, where h is layer depth and subscript u refers to the upper layer and subscript l refers to the lower layer. The bulk heat balance for the two reservoirs is:

$$\frac{d}{dt}(\forall_u H_u) = -\frac{d}{dt}(\forall_l H_l) = A \left(\kappa_T \Delta T + H_l \frac{dh_u}{dt} \right), \quad (5)$$

where \forall = volume = hA , A = area, $H = \rho c_p T$ = heat content per unit volume, c_p = constant pressure specific heat and κ_T = interfacial heat transfer coefficient. A heat transfer coefficient is introduced because the interfacial thickness is unknown and, ideally, approaches zero. However, this term represents molecular diffusion across the interface, as will be demonstrated below. The entrainment term represents the contribution of turbulence to the interfacial flux. Since A is constant, (5) is rearranged to obtain:

Table 1. Data summary for salt-stratified tests

Test	ΔS (%)	Ri	$E (\times 10^3)$
S1	0.5	2.89	9.36
S2	0.4	2.07	16.5
S3	0.7	3.82	8.06
S4	0.9	4.80	5.88
S5	0.6	3.11	6.90
S6	7.3	39.9	0.872
S7	5.2	28.2	1.19
S8	3.8	20.7	0.919
S9	2.9	15.6	2.21
S10	8.9	48.8	0.788
S11	2.3	12.6	1.30
S12	5.5	30.0	1.30
S13	8.2	44.9	0.670
S14	5.9	32.2	0.861
S15	2.6	14.4	1.93
S16	1.5	8.03	3.45

Table 2. Data summary for double-diffusive tests

Test	ΔS (%)	ΔT (°C)	R_p	Ri	E ($\times 10^3$)	κ_T ($W m^{-2} C^{-1}$)	κ_S ($m s^{-1} \times 10^6$)	F_H ($W m^{-2}$)	F_S ($\% m s^{-1} \times 10^6$)	R_F	F_H/H_S
D1	2.7	1.2	47.9	14.5	2.75	—	—	—	—	—	—
D2	0.4	2.6	2.26	1.10	14.5	85.3	3.3	222	1.2	0.68	0.50
D3	0.3	3.3	1.48	0.515	25.9	91.2	5.1	301	1.5	0.60	0.49
D4	14.9	14.2	19.0	77.1	0.494	54.6	—	775	—	—	0.15
D5	14.0	14.8	18.0	72.4	0.673	116.2	1.3	1720	18.0	0.79	0.32
D6	10.7	1.0	437	58.4	0.341	31.7	0.084	31.7	0.91	3.90	0.26
D7	9.6	2.5	103	52.0	0.494	48.3	0.75	121	7.2	7.49	0.29
D8	9.9	5.5	40.5	52.8	0.505	41.0	0.50	226	5.0	2.40	0.18
D9	10.7	3.8	56.4	57.3	0.486	49.1	0.25	187	2.7	1.70	0.25
D10	11.0	5.7	32.8	58.3	0.559	52.5	0.071	299	0.78	0.28	0.22
D11	6.3	1.2	161	34.4	0.635	39.7	0.065	47.6	0.41	1.17	0.31
D12	7.4	6.4	25.3	40.3	0.635	66.0	0.34	422	2.5	0.62	0.27
D13	7.8	3.7	42.2	41.4	0.722	45.5	—	168	—	—	0.23
D14	7.5	6.6	23.5	41.2	0.808	65.7	0.24	434	1.8	0.43	0.26
D15	7.5	4.2	35.7	39.5	0.932	55.5	—	233	—	—	0.27
D16	5.0	1.5	90.0	27.1	0.916	40.4	0.009	60.6	0.048	0.11	0.29
D17	4.8	2.5	54.3	25.9	1.39	44.4	—	111	—	—	0.26
D18	4.5	10.5	7.84	21.3	1.32	51.3	—	539	—	—	0.17
D19	3.0	3.0	25.0	15.7	1.77	45.4	—	136	—	—	0.25
D20	3.3	0.8	116	18.0	1.30	55.8	0.089	44.6	0.30	0.88	0.50
D21	3.3	11.8	4.97	14.4	2.45	69.8	0.20	824	0.66	0.07	0.21
D22	2.2	11.8	3.33	8.37	4.07	88.3	4.8	1042	11.1	0.89	0.27
D23	1.9	5.3	9.62	13.2	2.97	65.8	—	349	—	—	0.29
D24	1.1	1.9	17.9	5.72	3.53	58.6	0.31	111	0.34	0.40	0.38
D25	0.6	5.1	2.39	1.81	14.3	79.8	5.2	407	3.0	0.81	0.36

$$\frac{dH_u}{dt} = \frac{1}{h_u} \left[\kappa_T \Delta T + (H_l - H_u) \frac{dh_u}{dt} \right], \quad (6)$$

$$\frac{d}{dt} \Delta \rho_s = - \left(\frac{\kappa_s}{\zeta} + \frac{u_e}{h_u} \right) \Delta \rho_s, \quad (9)$$

and

$$\frac{dH_l}{dt} = - \frac{\kappa_T}{h_l} \Delta T. \quad (7)$$

Assuming $(\rho c_p)_s \approx \rho_0 c_p$ is constant, then subtracting (6) from (7) and dividing by $\rho_0 c_p$ results in:

$$\frac{d}{dt} \Delta T = - \left(\frac{\kappa_T}{\rho_0 c_p \zeta} + \frac{u_e}{h_u} \right) \Delta T. \quad (8)$$

where $\zeta = (h_u h_l) / (h_u + h_l)$. A similar analysis for salt stratification gives:

where $\rho_s = \rho S =$ salt density and $\kappa_s =$ interfacial salt transfer coefficient.

Values for κ_T and κ_s were found by matching (8) and (9) to experimental data for ΔT and ΔS , respectively, over the course of each experiment. This was done with an iterative numerical procedure using observed values for u_e (time-varying) and initial values for h_u , h_l , ΔT and $\Delta \rho_s$. Equations (8) and (9) were then solved using a forward-stepping finite difference procedure and κ_T and κ_s were chosen so that the final values of ΔT and $\Delta \rho_s$ were reproduced for each test.

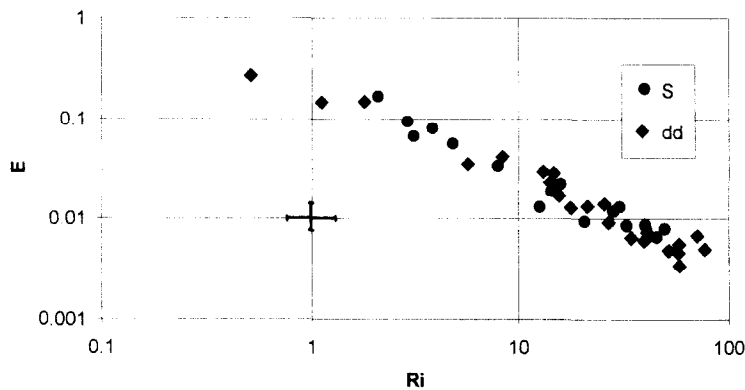


FIG. 2. Entrainment results for both salt stratified (S) and double-diffusive (dd) tests: bars indicate average experimental uncertainty.

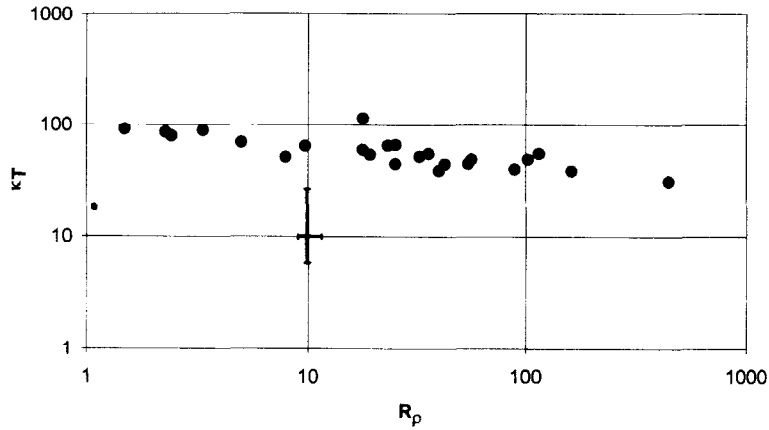


FIG. 3. Variation of interfacial heat transfer coefficient with stability ratio.

Estimates for κ_T and κ_S are listed in Table 2. A blank entry means the calculated value was negligibly small. An implicit assumption in this procedure is that the parameters remain constant during each test, though it is probably reasonable to expect some dependence on T and S . For example, both κ_T and κ_S appear to depend slightly on R_ρ , as shown in Figs. 3 and 4. R_ρ is chosen as the independent variable here since it has been shown in previous double-diffusive convection studies to strongly affect interfacial heat and salt fluxes. The increase in both κ_T and κ_S with lower R_ρ is probably an effect of the weaker interface. At this point it is not clear how varying values for κ_T and κ_S could be incorporated in evaluating equations (8) and (9) and the available data do not warrant such an exercise. However, the assumption of constant coefficient values for each test should not affect the results significantly.

It can be shown that the values obtained for κ_T and κ_S are consistent with molecular diffusivity values, as follows. The interfacial heat flux is $F_H = \kappa_T \Delta T$ and interfacial salt flux is $F_S = \kappa_S \Delta S$. The interfacial heat flux resulting from molecular diffusion is $\kappa(\partial T/\partial z)$, where κ = thermal conductivity and $(\partial T/\partial z)$ is the

vertical temperature gradient across the interface. Molecular salt flux is $k_S(\partial S/\partial z)$, where k_S = molecular salt diffusivity. If the interface is small the gradients may be assumed as approximately constant, $(\partial T/\partial z) \cong \Delta T/\delta_T$ and $(\partial S/\partial z) \cong \Delta S/\delta_S$, where δ_T and δ_S are the thicknesses of the diffusive interface associated with temperature and salinity stratification, respectively. Equating the flux expressions then shows $\delta_T = \kappa/\kappa_T$ and $\delta_S = k_S/\kappa_S$. With values for κ_T ranging between about 35 and 100 $\text{W m}^{-2} \text{ }^\circ\text{C}^{-1}$ and using a nominal value of $\kappa = 0.59 \text{ W m}^{-1} \text{ }^\circ\text{C}^{-1}$, then $\delta_T = 0.59\text{--}1.69 \text{ cm}$. Although detailed measurements of interfacial thicknesses were not made for all the tests, the probe profiles and also visual observations indicated an interfacial thickness in the order of 1 cm, well within the calculated range. Values for κ_S are all small and show greater scatter. From Fig. 4 an average value is taken as $2.5 \times 10^{-7} \text{ m s}^{-1}$. Then, $k_S = 1.4 \times 10^{-9} \text{ m}^2 \text{ s}^{-1}$, the result is $\delta_S = 0.56 \text{ cm}$. This is slightly smaller than observed, but of the same order of magnitude.

Equation (8) and (9) can be combined to calculate changes in the net density step by noting that $\Delta\rho = \rho_0(-\alpha\Delta T + \beta\Delta S)$. Dividing (9) by ρ and assuming α and β to be constant:

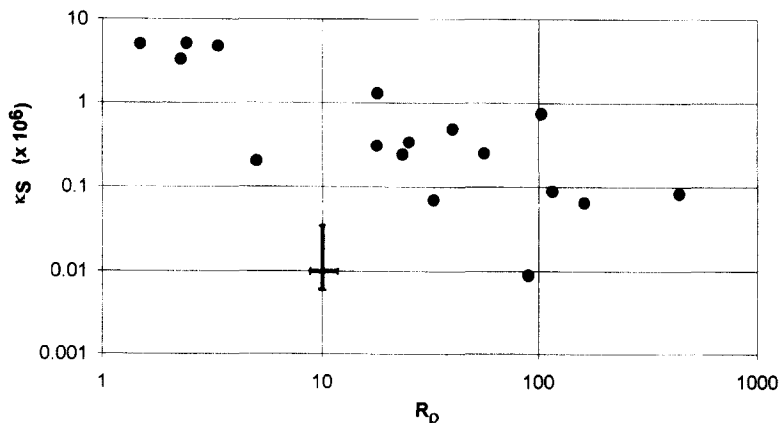


FIG. 4. Variation of interfacial salt transfer coefficient with stability ratio.

$$\frac{d}{dt} \left(\frac{\Delta\rho}{\rho_0} \right) = \frac{1}{\zeta} \left[\frac{\alpha F_H}{\rho_0 c_p} (1 - R_F) \right] + \frac{u_e}{h_u} \alpha \Delta T (1 - R_p). \tag{10}$$

This last result is essentially a generalization of expressions derived previously [13, 20], by including the contribution due to entrainment. Note that in Crapper's [13] experiments both layers were stirred and maintained at constant and equal depths, so $u_e = 0$ and $\zeta = h/2$. With these substitutions (10) reduces to his result [his equation (6)]. The entrainment contribution in equation (10) is always negative since $R_p > 1$. However, the flux contribution can be positive or negative, depending on the value of R_F relative to 1. Values for R_F are listed in Table 2 and plotted in Fig. 5 as a function of R_p . No simple relationship between these two parameters is indicated, though it appears that R_F generally increases with R_p . Curves for several previous models are also shown and these, along with the scatter seen in these data, will be discussed in the following section.

One other result of interest concerns the non-dimensional heat flux, F_H/H_{sp} , where H_{sp} is the equivalent heat flux that would be expected if the interface were replaced with a solid, perfectly conducting plane. Turner [1] first introduced this concept and defined H_{sp} by:

$$H_{sp} = 0.084 \rho_0 c_p k_T \left(\frac{g\alpha}{\nu k_T} \right)^{1/3} \Delta T^{4/3}, \tag{11}$$

where ν = kinematic viscosity. A number of earlier studies in unstirred systems were reviewed by Atkinson *et al.* [14], who showed that the empirical expression, $F_H/H_{sp} = 1.09(R_p - 1)^{-1.14}$, provided a good fit for all the data with R_p between 3 and 30. From Fig. 6, however, it is seen that this relationship underpredicts heat flux except for low R_p . Furthermore, the present dimensionless heat flux values are relatively constant, with an average value of 0.29. This result seems reasonable since F_H/H_{sp} is approximately

proportional to $\kappa_T/\Delta T^{1/3}$ [assuming other variables in equation (11) are constant]. Thus, there is a weak dependence on ΔT , but as previously noted there is also a slight increase in κ_T for higher ΔT (i.e. lower R_p —see Fig. 3). While the conclusion is considered tentative at this time, it appears that the effect of increasing ΔT is approximately balanced by an increase in κ_T , so that F_H/H_{sp} is about constant. This balance is apparently not maintained in a non-stirred system.

4. DISCUSSION

In order to discuss the effects of double-diffusive stratification on grid-induced entrainment and the effect of stirring on interfacial fluxes it is first useful to consider time-scales for these processes. Previous models of a diffusive interface have considered mixed or stratified layers on either side of the interface and finite or zero density steps. In most of these a stably stratified fluid is heated from below and convective mixing provides a well-mixed lower layer. Linden and Shirtcliffe [4] and Fernando [20] assumed that gradients vanished in both the upper and lower layers. Other studies [18, 19] assumed zero gradients in the lower layer and also no step at the interface ($\Delta\rho = 0$). For an initially stratified system with stirring in one of the layers these conditions are possible only if u_e is very small; otherwise a density step will form. Most of these models assume a sharp interface as an initial condition.

With time, diffusive boundary layers develop at the edges of the interface. This process continues until the layers are swept away, either because of the development of instabilities [4] or because of entrainment by turbulent eddies [20]. Which of these processes actually occurs depends on a comparison of relevant time-scales. Fernando [20] argued that the entrainment occurred on a shorter time-scale and thus would control mixing. In a subsequent study [19] it was

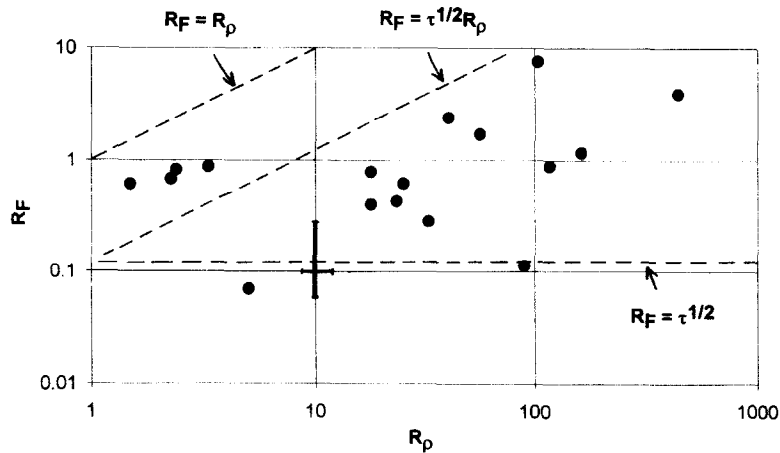


FIG. 5. Dependence of interfacial flux ratio on stability ratio; also shown are three formulae relating R_F and R_p .

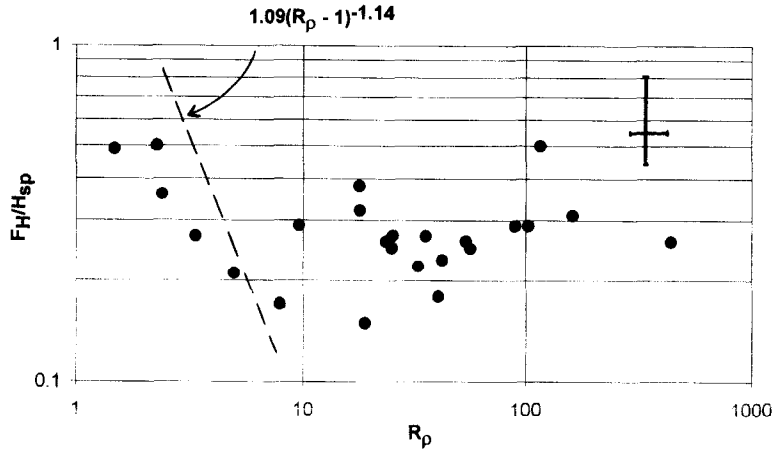


FIG. 6. Variation of non-dimensional heat flux with stability ratio: the curve shows the empirical result reported by Atkinson *et al.* [3].

shown that this result was valid for the given experimental conditions, using the instability time-scale developed by ref. [18]. However, this time-scale is not applicable for the present tests since it depends on non-zero gradients in the layer being entrained. Atkinson *et al.* [14] developed an instability time-scale based on Linden and Shirtcliffe's model [4]:

$$t_c = \left\{ \frac{1}{\pi k_T} \left[\frac{\nu Ra_c}{g \alpha \Delta T (1 - \tau^{1/2})^3} \right]^2 \right\}^{1/3}, \quad (12)$$

where Ra_c is a critical Rayleigh number for the development of convective instability and has a value of about 1640. This time-scale may be compared with the eddy scale [20]:

$$t_c = \frac{l_1}{u_1}. \quad (13)$$

In other words, for an initially unstirred system to which mixing energy is slowly added, the stirring is expected to start to have an impact on interfacial fluxes when $t_c \simeq t_c$. As mixing intensity is further increased t_c will decrease and the stirring will dominate the transport process.

Crapper's [13] data provide a means of checking this hypothesis, noting that the conditions in his experiment were similar to those assumed in ref. [4], so that t_c given by equation (12) is applicable. First, the time-scale ratio is:

$$\frac{t_c}{t_c} = \left(\frac{u_1}{l_1} \right) t_c = \lambda \left(\frac{u_c}{l_1} \right) t_c, \quad (14)$$

where $\lambda = u_1/u_c$ and u_c is a velocity scale associated with convective motions generated by bottom heating. In Crapper's experiments the quantity (u_c/l_1) was constant. If the time-scales are comparable, $t_c \simeq t_c$, then λ may be calculated as a function of t_c . Using u_c and l_1 from Crapper's tests, ΔT between 3 and 10°C and representative values for the other parameters in equation (12), λ is found to be between 0.07 and 0.15.

From Crapper's results (his Fig. 5), a clear effect of the grid is seen at $\lambda \simeq 0.1-0.2$, although the fluxes are not completely dependent on the grid-mixing until $\lambda \geq 1$. Thus, the evaluation of mixing mechanisms in terms of time-scales appears to be supported by Crapper's data.

For the present tests $t_c = 2.7$ s, while the lowest value of t_c is 24 s. Therefore, interfacial convective instabilities should not be present and this explains the lack of effect of double-diffusive stratification on the entrainment results. In order for convective velocity to have an effect, experiments would have to be conducted with relatively high ΔT (to reduce t_c) and low stirring intensities. Increasing ΔT decreases the net density step at the interface, thus changing Ri slightly, with an accompanying change in E . A stronger effect, however, is a local weakening of the interface so that fluid becomes more susceptible to mixing. The model of Zangrando and Fernando [19] assumes this sort of mechanism and also that the sweeping away of the diffusive boundary layer leads to entrainment. In other words, $u_c \approx l_d/t_c$, where l_d is a diffusive length-scale estimated from $l_d \approx (kt_c)^{1/2}$ (k is diffusivity of either salt or heat). It is then easily shown that $E \approx Pe^{-1/2}$, where $Pe = u_1 l_1/k$ is the Peclet number. Zangrando and Fernando's analysis also gives this result, though they account for the double-diffusive boundary layer structure in greater detail. In the present experiments the entrainment rate is faster because of the added mixing energy from the oscillating grid. Because of the relatively short time-scale for the eddies it appears that there is not an appreciable effect of the diffusing temperature profile on E . As above, this process would presumably be more visible for higher ΔT and lower stirring intensity.

Referring to Fig. 5, it is clear that the present results do not support a simple relationship between R_F and R_p —another variable must be involved. The theoretical curves shown in this figure include $R_F = \tau^{1/2}$ [3, 4], and $R_F = \tau^{1/2} R_p$ [2, 20]. Both of these models were

developed for non-stirred systems. With a few exceptions at low R_ρ , the present data fall between these two lines. At the other extreme, for a system in which interfacial mixing is completely dominated by entrainment, the flux ratio will equal the buoyancy ratio ($R_F = R_\rho$) and this line is also shown. Now, Crapper's [13] data for R_F show a dependence on λ as well as on R_ρ . At low λ the curve is quite flat, with little dependence on R_ρ . The slope (proportionality between R_F and R_ρ) then increases with increasing λ (his Fig. 3). Since λ is a measure of the relative strength of stirring, it seems reasonable that Ri might be used to try to collapse the present data for R_F . The reasons for choosing this parameter include: (i) Ri is also a measure of the relative strength of stirring; and (ii) E clearly depends on Ri . Thus, at small Ri , R_F should approach R_ρ since entrainment is proceeding relatively quickly. At large Ri , R_F should be less than R_ρ and in the limit of very large Ri (when $E \rightarrow 0$), R_F should tend to the values observed for non-stirred systems.

In Fig. 7 the ratio R_F/R_ρ is plotted as a function of Ri . This ratio takes a maximum value of 1 when Ri is small. Also, by substituting from equation (1):

$$\frac{R_F}{R_\rho} = \frac{\kappa_S}{\kappa_T/\rho c_p} \tag{15}$$

Therefore, R_F/R_ρ is equivalent to the ratio of salt and heat transport coefficients. With this interpretation in mind, it is to be expected that R_F/R_ρ should decrease with increasing Ri since there is less energy available for lifting salt and contributing to κ_S (κ_T remains relatively higher because of the greater diffusivity for heat). As stirring energy decreases, a point may be reached where $t_e > t_c$ and then a possible contribution of convective velocity to Ri would have to be considered. If buoyant convection provides enough energy for scouring the boundary layers, then the lower limit of $R_F/R_\rho = \tau^{1/2}$ suggested by Fernando [20] should be reached. However, if the energy is insufficient then the limiting condition would be governed by interfacial fluxes driven by boundary layer instability and R_i may approach a constant value (e.g.

$\tau^{1/2}$). In this case R_F/R_ρ would not necessarily have a minimum.

Although there is still some scatter in Fig. 7, particularly at large Ri , it appears that R_F/R_ρ does indeed decrease with increasing Ri . It is also worth noting that Crapper's [13] data are consistent with a decrease in R_F/R_ρ with increasing Ri . Four values of this ratio that may be deduced from his data are 0.18, 0.11, 0.068 and 0.048 (in order of increasing Ri). Unfortunately, it is not possible to calculate Ri directly from the information given in that paper, but these values are similar to much of the present data. This result is also consistent with a further interpretation of the ratio R_F/R_ρ , by assuming that the transfer coefficients are equivalent to molecular diffusive fluxes across the interface, as previously suggested. Then, with $\kappa_S = k_S/\delta_S$ and $\kappa_T/\rho c_p = k_T/\delta_T$, equation (15) becomes:

$$\frac{R_F}{R_\rho} = \tau L, \tag{16}$$

where $L = \delta_T/\delta_S$. Since τ does not change much, a reduction in R_F/R_ρ corresponds with a decrease in L . If the diffusive thicknesses are determined from:

$$\delta \simeq (kt)^{1/2}, \tag{17}$$

where t is time from an initial condition of zero thickness, then $L \simeq \tau^{-1/2}$ and $R_F/R_\rho = \tau^{1/2}$, which is Fernando's [20] result. However, the temperature profile cannot diffuse ahead of the salt profile indefinitely—it will be limited by the development of convective instability. Then it may be expected that L would be somewhat less than $\tau^{-1/2}$ since δ_S could increase, relative to δ_T .

It is clear from Fig. 7 that R_F/R_ρ reaches values less than $\tau^{1/2}$. From the above discussion, this appears to be a result of different interfacial thicknesses than those assumed in the theoretical development. For example, Fernando [20] predicted interfacial thickness from equation (17), using $t = t_c$, where t_c corresponds with the layer stirred less vigorously (this is related to the fact that the interface will grow more into the layer

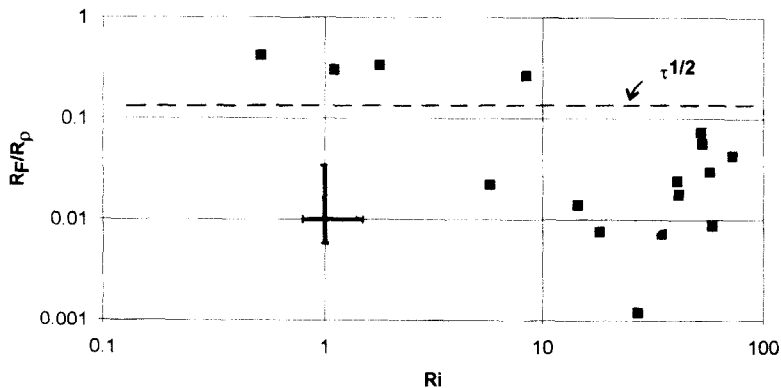


FIG. 7. Variation of the ratio R_F/R_ρ with Richardson number.

with less stirring intensity and gives a higher value for t_c). For the present tests t_c is estimated from the convective velocity-scale for the lower layer, which is determined from the net interfacial buoyancy flux:

$$u_c = \left[gh_l \left(\frac{\alpha F_H}{\rho_o c_p} - \beta F_S \right) \right]^{1/3} \\ = \left[gh_l \frac{\alpha F_H}{\rho_o c_p} (1 - R_F) \right]^{1/3}. \quad (18)$$

This results in $u_c = 0.1\text{--}0.2 \text{ cm s}^{-1}$ and $t_c = 175\text{--}350 \text{ s}$, giving $\delta_T = 0.5\text{--}0.7 \text{ cm}$ and $\delta_S = 0.05\text{--}0.07 \text{ cm}$. While detailed interfacial thickness measurements were not made in these tests, profile data and observations suggest that slightly thicker interfaces were present, especially for the salinity profile. It is possible that the weak convection in the lower layer did not have sufficient energy to effectively scour the interface, so that the interfacial thickness was larger and the diffusive flux smaller than in the theoretical model. Since this effect is more pronounced with the salt profile, R_F values are less than those predicted by the theory (i.e. $R_F/R_\rho < \tau^{1/2}$).

5. CONCLUSIONS

The main results from this study show: (1) that the unstable temperature gradient has a negligible effect on salt-stratified entrainment, at least for the parameter range considered; and (2) that the grid-stirring has a significant impact on the interfacial fluxes of heat and salt. The first result is not entirely surprising since many of the experimental values for R_ρ are larger than would normally be expected for double-diffusive effects to be important. It should also be noted that for small R_ρ , $\Delta\rho \rightarrow 0$ and Ri is also small. In this region molecular effects are considered to be secondary to turbulent mixing, so it may be argued that diffusive stratification should not have an effect on net interfacial movement (compared with salt stratification) for all values of R_ρ (> 1) and Ri . However, experiments should be performed to confirm this result, probably with greater ΔT and/or lower stirring intensity than in this study.

The second result was explained in terms of the scouring of the interfacial diffusive boundary-layers resulting from the grid stirring. This prevents instabilities from developing so that there is no convection in the upper layer. Maintaining a relatively sharp interface also results in increased interfacial fluxes, for both heat and salt, compared with values reported for unstirred diffusive systems. Unlike unstirred systems, there is no simple relationship between R_F and R_ρ and it is suggested that Ri should also be considered. The ratio R_F/R_ρ , chosen because of its interpretation as the ratio between salt and heat interfacial transport coefficients, appears to depend on Ri , decreasing as Ri increases. Although mechanistic arguments support this type of relationship, there is some scatter in

the present data and further experiments are needed to determine the exact relationship. This would be a worthwhile direction to pursue for field applications since in many situations external sources of mixing are present.

The present study confirms that a comparison of time-scales for eddy motions and for growth of boundary layer instability provides a valid criterion for deciding which mechanism is more important in sweeping away the diffusive boundary layers and contributing to interfacial fluxes. This comparison was suggested previously [14, 19, 20] and is shown here to be valid for grid-mixing studies as well. This type of comparison should be helpful in evaluating results for larger Ri , where t_c would be larger.

Acknowledgements—The raw data used in this report were collected as part of the doctoral dissertation of the author. That project was supported by the National Science Foundation, Grant No. CEE-8119384, and by the Department of Energy, through the Solar Energy Research Institute, subcontract XX-3-03066-1. The author thanks Leonardo Damiani, who assisted with much of the LDA measurements, Larry Deshaine for his help in setting up the experimental apparatus, and especially his former advisors, Donald Harleman, Eric Adams and W. Ken Melville, for their invaluable help in carrying out the original experiments and analyses. Finally, the Lady Davis Fellowship Trust Fund (Jerusalem) provided support for the present effort.

REFERENCES

1. J. S. Turner, The coupled turbulent transport of salt and heat across a sharp density interface, *Int. J. Heat Mass Transfer* **8**, 759–767 (1965).
2. J. S. Turner, T. G. L. Shirtcliffe and P. G. Brewer, Elemental variations of transport coefficients across density interfaces in multiple-diffusive systems, *Nature* **228**, 1083 (1970).
3. T. G. L. Shirtcliffe, Transport and profile measurements of the diffusive interface in double diffusive convection with similar diffusivities, *J. Fluid Mech.* **57**, 27 (1973).
4. P. F. Linden and T. G. L. Shirtcliffe, The diffusive interface in double-diffusive convection, *J. Fluid Mech.* **87**, 417–432 (1978).
5. H. J. S. Fernando, Turbulent mixing in stratified fluids, *Ann. Rev. Fluid Mech.* **23**, 155–193 (1991).
6. X. E. and E. J. Hopfinger, On mixing across an interface in stably stratified fluid, *J. Fluid Mech.* **166**, 227–244 (1986).
7. H. J. S. Fernando and R. R. Long, The growth of a grid-generated turbulent mixed layer in a two fluid system, *J. Fluid Mech.* **133**, 377–395 (1983).
8. I. A. Hannoun and E. J. List, Turbulent mixing at a shear-free density interface, *J. Fluid Mech.* **189**, 211–234 (1988).
9. E. J. Hopfinger and J. A. Toly, Spatially decaying turbulence and its relation to mixing across a density interface, *J. Fluid Mech.* **78**, 155–175 (1976).
10. T. J. McDougall, Measurements of turbulence in a zero-mean-shear layer, *J. Fluid Mech.* **94**, 409–431 (1979).
11. R. I. Nokes, On the entrainment rate across a density interface, *J. Fluid Mech.* **188**, 185–204 (1988).
12. J. S. Turner, The influence of molecular diffusivity on turbulent entrainment across a density interface, *J. Fluid Mech.* **33**, 639–656 (1968).
13. P. F. Crapper, Fluxes of heat and salt across a diffusive interface in the presence of grid generated turbulence, *Int. J. Heat Mass Transfer* **19**, 1371–1378 (1976).

14. J. F. Atkinson, E. E. Adams and D. R. F. Harleman, Double-diffusive fluxes in a salt gradient solar pond, *J. Solar Energy Eng.* **110**, 17–22 (1988).
15. P. F. Linden, A note on the transport across a diffusive interface, *Deep-Sea Res.* **21**, 283–287 (1974).
16. A. Murota and K. Michioku, Stability and vertical mixing in double-diffusive stratification system composed of heat-salt complex, *J. Hydrosoci. Eng.* **1**, 53–63 (1983).
17. J. R. Hull and J. M. Mehta, Physical model of gradient zone erosion in thermohaline systems, *Int. J. Heat Mass Transfer* **30**, 1026–1036 (1987).
18. M. J. Witte and T. A. Newell, A thermal burst model for the prediction of erosion and growth rates of a diffusive interface, ASME paper 85-HT-31, Heat Transfer Conference, Denver, CO (1985).
19. F. Zangrando and H. J. S. Fernando, A predictive model for the migration of double-diffusive interfaces, *J. Solar Energy Eng.* **113**, 59–65 (1991).
20. H. J. S. Fernando, Buoyancy transfer across a diffusive interface, *J. Fluid Mech.* **209**, 1–31 (1989).
21. J. F. Atkinson, L. Damiani and D. R. F. Harleman, A comparison of velocity measurements using a laser anemometer and a hot film probe, with application to grid-stirring entrainment experiments, *Phys. Fluids* **30**, 3290–3292 (1987).
22. J. F. Atkinson, E. E. Adams, W. K. Melville and D. R. F. Harleman, Entrainment in diffusive thermohaline systems: application to salt gradient solar ponds. Technical report no. 300, Ralph M. Parsons Lab., Department of Civil Engineering, MIT, Cambridge, MA (1985).
23. M. W. Kellogg, Co., *Saline Water Conversion Engineering Data Book*. Prepared for the Office of Saline Water, U.S. Department of the Interior (1965).
24. D. J. Carruthers and J. C. R. Hunt, Velocity fluctuations near an interface between a turbulent region and a stably stratified layer, *J. Fluid Mech.* **165**, 475–501 (1986).
25. S. M. Thompson and J. S. Turner, Mixing across an interface due to turbulence generated by an oscillating grid, *J. Fluid Mech.* **67**, 349–356 (1975).